Quantitative Velocity Field Measurements in Reduced-Gravity Combustion Science and Fluid Physics Experiments

Paul S. Greenberg
Mark P. Wernet
NASA-Lewis Research Center
Cleveland, OH 44135

Abstract

Systems have been developed and demonstrated for performing quantitative velocity measurements in reduced-gravity combustion science and fluid physics investigations. The unique constraints and operational environments inherent to reduced-gravity experimental facilities pose special challenges to the development of hardware and software systems. Both point and planar velocimetric capabilities are described, with particular attention being given to the development of systems to support the International Space Station laboratory. Emphasis has been placed on optical methods, primarily arising from the sensitivity of the phenomena of interest to intrusive probes. Limitations on available power, volume, data storage, and attendant expertise have motivated the use of solid-state sources and detectors, as well as efficient analysis capabilities emphasizing interactive data display and parameter control.

1. Introduction

The availability of microgravity facilities of increased duration combined with manned presence offers unprecedented opportunities to conduct experimental investigations of both a fundamental and applied nature. The new International Space Station (ISS) laboratory fosters unique issues relating to the design and operation of experiment-related systems. In particular, significantly increased operational lifetimes, constraints on upmass capabilities, limitations on both in-situ data storage and communications bandwidths, and issues relating to the dispensation of crew expertise and availability present new challenges to the development of instrumentation systems.

The measurement capability described here concerns the quantitative determination of velocity fields. A primary attribute of phenomena occurring under reduced gravity conditions is the significantly diminished role of buoyancy-induced convective motions. Systems with inherent density gradients induced by exothermic reactions, externally imposed heat fluxes, or hydrostatic pressure exhibit marked differences relative to their normal gravity counterparts. The role of buoyancy insofar as complicating analytical and numerical models, and masking relatively weaker mechanisms such as diffusion, surface tension, and radiative transfer has long been recognized. A more complete discussion is beyond the present scope, and the reader is referred to existing reviews on the subject.[1, 2] For the purposes here, it is sufficient to note that for a vast array of phenomena of scientific interest, the reduction in gravitational influences is most noticeably observed by differences in the resulting flow fields. Because these flow fields mediate heat and mass transfer, velocity fields are among the single most important observable in microgravity science investigations.

Diagnostic methods for velocity field determination are at once segmented into point and planar techniques. Neither is inherently superior, but rather serve as complementary capabilities. Particular advantages are driven by the specifics of a given application, as will be discussed. It is also important to recognize that reduced-gravity phenomena are generally ill-suited to intrusive probes, e.g. hot wire anemometers, pitot-static tubes, or vane-type devices. Removal of the comparatively vigorous action of buoyancy-induced convection leaves in its stead systems dominated by the weaker mechanisms previously described. Further, many systems of interest involve the determination of limiting behaviors or conditions, such as combustion flammability limits, or configurational stability in fluid systems. In such cases, it has been seen that intrusive probes may unacceptably alter the observed limiting behaviors. For these reasons, optical diagnostics are preferable.

Point and field measurement capabilities have been developed using the methods of Laser Doppler Velocimetry (LDV) and Particle Image Velocimetry (PIV), respectively. Considerable attention has been devoted over the past decade to the development of hardware systems and analysis capabilities supporting both methods.[3, 4] The emphasis reported here involves the development of systems compatible with operation within the ISS laboratory environment.

2. Laser Doppler Velocimetry Systems

In brief, LDV relies on the doppler shift of incident radiation upon scattering. In common with PIV, general practice involves the introduction of small seed particles (~1 μm) to serve as scattering centers. These particles must track the flow with suitable fidelity, thereby constraining the maximum allowable diameter for a given density, and hence the magnitude of the scattered signal for a specified optical source strength. Although molecular scattering for velocimetric applications has been utilized, this approach is generally impractical. Molecular scattering cross sections are weaker by some twenty orders of magnitude, and thermal velocity broadening is on the order of one GHz at standard temperature and pressure.

The configuration adopted here, by far the most common, is the dual-doppler or heterodyne method.[3] Scattered contributions from two simultaneous input beams are combined in a square law detector such that the carrier frequency corresponding to the incident radiation ($\sim 10^{14}$ Hz) is removed by heterodyning, leaving only the lower frequency residual beat frequency. This beat frequency is proportional to the velocity magnitude, having a value on the order of 10^5–10^6 Hz/m/sec for most systems of interest. Useful attributes of LDV are its high spatial resolution and large measurement bandwidth. For the systems described here, the transverse spatial dimensions of the optical probe volume are roughly 75 microns, and independent measurements of velocity can be performed at rates of 100K samples/second. These features promote LDV for applications involving small scale spatial features and/or for the determination of turbulence spectra.

Optimizing the optical configuration involves a balance between several system variables. This is at once seen from the relationship for peak optical signal-to-noise ratio (SNR):

$$\mathrm{SNR}_{peak} = \frac{\pi^2}{256}\frac{\eta_q P_0}{h\upsilon_0 \Delta f}\left(\frac{D_a D_c^{-2}}{f_c f}\frac{d_{pi}}{\lambda}\right)^2 G_i \overline{V}_i$$

The variables of significance here are delineated as follows. While the detected SNR is linear in source strength, P_0, more significant is the squared dependence on transmission and collection f numbers as conveyed through the quantities D_c^{-2}/f and D_a/f_c respectively. $\overline{V}$, the particle visibility function, expresses the modulation depth of the scattered signal, and has as its argument the ratio of the seed particle diameter to the spacing of constant phase planes in the probe volume. For dual-beam systems with narrow convergence angles, the visibility can be expressed as a first order Bessel function. [5] The rapid decay of J_0 dominates the expression for SNR with increasing particle diameter, limiting the useful range to roughly a few microns and below. The dependence on particle scattering cross section is denoted by G_i, normalized by the geometric cross section, proportional to d^2_{pi}. Once an upper limit on particle size has been determined from hydrodynamic considerations, the general design approach involves minimization of system f numbers to the degree practical, iterating between particle size and input convergence angle to optimize the scattering cross section visibility product, then employing sufficient source strength to overcome the noise equivalent power (NEP) of the detector and its associated amplifiers.

Constraints on available power and volume have promoted approaches based on both solid-state laser sources and detectors. The conversion efficiency and compactness of semiconductor diode lasers would appear to favor these devices, however other considerations may be involved. True single-mode output is seldom achieved, and active thermal control is required to even approximate this condition. Sub-millimeter coherence lengths typically result, often complicating the optical design by virtue of pathlength matching requirements. The highly astigmatic output necessitates additional corrective elements. Regardless, diffraction-limited performance is rare, affecting both the tightness of focus, as well as the desired phase stationarity at the waist. In this case, the resulting curvatures artificially appear as gradients in velocity space.[7] More deleterious is the near complete loss of coherence caused by the onset of chaotic modal regimes in the presence of even vestigial back reflections. [8] While shorter wavelength lasers, i.e. visible, are desired to exploit k^4 scattering dependence, Faraday isolators in this region are larger than the remaining optical/thermal package itself. Costly distributed Bragg reflector lasers mediate these considerations only to an extent, and remain limited in available wavelengths and output powers. Semiconductor lasers will surely experience continued improvements, and remain of considerable interest as building blocks for single-chip integrated optical assemblies. At present, however, the complexity of optically corrected, thermally stabilized semiconductor sources makes solid-state lasers an attractive alternative. The latter are becoming available in packages of similar dimensions, while providing inherently superior optical characteristics.

A number of LDV optical configurations have been designed for use in the NASA reduced-gravity facilities. Although the context here concerns the ISS, the overall list of facilities also includes ground-based drop towers, sounding rockets, and reduced-gravity parabolic aircraft flights. As an example, a single-component system was constructed from a 15 milliwatt Fabry-Perot laser outputting at 780 nanometers. The entire package, including detector, preamplifier, current driver, and thermal control circuitry measures 56 millimeters in diameter and 200 millimeters in length.[6] For this system, residual source astigmatism remains incompletely corrected, resulting in artificial spectral broadening of approximately three percent across the axial sample volume extent. The aforementioned effect of optical feedback induced instability is additionally problematic.

In certain instances, semiconductor lasers can provide suitable performance, as in the following illustration. In this case, astigmatic correction is provided by microlenses directly bonded to the diode output facet.[9] The steep curvature of the microlens acts to effectively isolate the cavity from back reflections, and the improved correction reduces residual broadening to roughly one percent. A two component system employing color-based channel separation was constructed using a pair of these devices operating at 680 and 780 nanometers. The requirement to spatially match the probe volumes adds to the overall system complexity through the addition of mode matching and steering optics. In this case, a pair of avalanche photodiode detectors were fabricated with fiber optic pigtails to allow configurational flexibility. Continued refinements to this system presently center on provisions for directional discrimination. For reasons described above, a compact, ring-doubled, diode-pumped Nd:YAG laser is being evaluated as a replacement for the semiconductor sources now in use.

The estimation of velocity from the observed doppler signals requires dedicated signal processing capabilities, the development of which has been actively pursued by numerous investigators.[3] The system described here employs true 32-bit burst spectral processing with coincident threshold amplitude and SNR triggering.[10] The resulting processor is configured as a pair of 16-bit PC bus cards, permitting it to be housed in relatively modest platforms.

The implementation of signal processing and data storage capabilities is an important issue for ISS systems development. Virtually all experiments performed on orbit are ultimately constrained by limited telecommunication bandwidths. Current estimates indicate downlinked data streams on the order of 6 Mb/sec with access duty cycles on the order of fifty percent. While flight crews are impressively capable and well trained, the number of experiments alone will outpace the ongoing, interactive expertise required to conduct them. In situ processing is therefore highly advantageous for limiting data downlink requirements, but severe restrictions on available crew time and experiment-specific consumables motivate the need for rapid data validation and efficient user interfaces. To this end, the processor described here provides the user with an ensemble of real-time interactive interfaces. These include: i) oscilloscope-like raw signal representation with overlayed amplitude trigger thresholds; ii) derived frequency and SNR overlayed with system bandwidth and SNR acceptance threshold; iii) velocity-time histograms with instantaneous data rate; and iv) mean velocity, pdf's, moments, and Reynolds stresses. These features have evolved in response to the desire for optimizing data yield and quality by providing clear targets and informative status indicators. Further, the implementation of processor functions and displays through programmed DSP modules allows rapid alterations and additions via uplinked software commands.

Several examples of the described graphic user interfaces are depicted in figure 1. Panel (a) illustrates a single-shot doppler burst from the two-component system discussed above. Also evident is the interactively controlled amplitude trigger threshold level, as well as derived spectral quantities. In (b) is shown the V-t histograms, pdf's, means, etc. Panel (c) shows a plot of axial velocity vs. downstream position for a premixed turbulent flame operating under both normal and reduced-gravity conditions. The effect of buoyant acceleration is clearly visible in the former.

3. Particle Image Velocimetry Systems

PIV is generally implemented in the form of a planar measurement technique, wherein a pulsed laser light sheet is used to illuminate a flow field seeded with tracer particles in similarity with LDV. The positions of the particles are photographically recorded at each instant the light sheet is pulsed or shuttered. While film-based imaging media are still employed for reasons of spatial resolution, the impracticality of chemical processing promotes electronic media for ISS applications. CCD cameras are reliable, compact, low cost and have low power requirements. For low velocity liquid flows and/or small fields of view, CW light sources can be chopped, or used in combination with an electronically shuttered CCD. Pulsed sources make more efficient use of available photon densities, and are invariably required for applications involving higher velocities. Pulsed sources compatible with ISS operations are now becoming available. The data processing consists of determining either the average displacement of the particles over a small interrogation region in the image (correlation processing) or the individual particle image displacements (particle tracking). Knowledge of the time interval between light sheet pulses then permits computation of the flow velocity. While PIV offers the advantage of simultaneous full-field interrogation and thus the determination of non-stationary spatial structures, it does not provide the spatial resolution and temporal responsivity achievable with LDV. In certain instances, optical access (e.g. entrance or exit window locations, proximity to an opaque surface, etc.) may mandate a particular approach.

PIV has been previously demonstrated in reduced gravity fluid physics and combustion experiments.[11, 12] In these examples, particle tracking was employed to process video-rate data records. As will be discussed in more detail, particle tracking is best suited to low velocity, sparsely seeded flows, and provides moderate accuracy velocity estimates on the order of 5-10%. The principal issues of concern for implementing a PIV system in the limited confines of the ISS are: i) light sheet generation; ii) flow seeding; iii) image recording and storage; and iv) post processing and data validation.

Examples of these concerns are reflected in the Surface Tension Driven Convection Experiment (STDCE), performed on the Space Shuttle in 1992. In this case, the relatively slow surface tension driven liquid phase velocities were accommodated by a 200 milliwatt CW diode laser illumination source. The output wavelength of 800 nanometers was chosen to correspond to the peak responsivity of the CCD imaging array. The use of video- rate image acquisition enabled the use of conventional 30 fps video tape recording systems. Further, video tape recording enabled experimental data to be collected over periods spanning several hours, while crew members were engaged in visually monitoring the quality of the particle image data being acquired. The relatively short mission duration allowed the recorded particle image data to be digitized and processed after the fact. As discussed, recording and post analysis does not represent a viable strategy for most ISS applications. Parenthetically, ISS data acquisition and storage provisions have supplanted previous analog video recording capabilities with all digital systems.

Particulate seeding of the flow focused mainly on the light scattering properties of the particles and their hydrodynamic behavior. Nominal 20 micron diameter alumina particles were selected for their large scattering cross section and their compatibility with the silicon oil flow in the STDCE. In comparison, alumina would not represent the seed material of choice for a terrestrial application, due to its large specific gravity and therefore high settling velocity. In a reduced-gravity environment, specific gravity concerns are eliminated, however particle agglomeration remains a concern. If the particles are dispersed in the fluid in a 1g environment, then the particles will rapidly settle out of solution. The particles must be prevented from agglomerating to permit effective redispersal on-orbit. From this perspective, it is important to understand the surface characteristics of the particles and their interaction with the fluid being used. Techniques to regulate and control the London-Van der Waal interparticulate forces may be required to avoid or minimize agglomeration.[13] ISS operations pose additional and peculiar challenges to the handling of seed materials. In many situations, the preparation of pre-seeded solutions or mixtures may precede actual usage by months, if not years, thus involving the investigation of stability over longer time frames. In addition, the introduction of material cannot exploit gravitational feed mechanisms, and techniques involving pressure feeding (i.e. compaction) of unstabilized powders are typically ill-fated. Further, safety considerations for manned spacecraft preclude the handling of incompletely contained fluids or particulates. Although not discussed in the previous section, seed particle disbursement under reduced-gravity conditions represents a unique problem in its own right, and significant efforts continue to be expended in this regard.

Certain experiment-specific considerations may also influence how a PIV system is configured. For example, the requirement of a constant wall temperature boundary condition in the STDCE necessitated a temperature jacket around the cylindrical test cell reservoir. Normally, the imaging optical axis is oriented normal to the plane of illumination. The constant wall temperature jacket precluded this arrangement, so an alternative viewing system was devised based on the Schiemplflug condition, a technique normally used to correct images obtained from aerial reconnaissance. The illuminated plane in the center of the fluid reservoir was viewed through a special lens element machined into the bottom of the reservoir. Viewing a tilted object through a normal camera lens arrangement requires an extremely large depth of focus to maintain focus across the entire image plane. By tilting the camera so that the plane of the object (the light sheet illumination plane), the median plane through the lens, and image plane (CCD sensor) all intersect at a common point, all points on the object plane are in-focus on the image plane. An artifact of the Schiempflug configuration is perspective distortion in the recorded images. A numerical correction algorithm was then developed to compensate for the perspective distortion in the data reduction of the PIV images. Figure 2 illustrates both raw data and derived velocity maps from the STS-50 Mission of STDCE. The data reduction was performed using similar algorithms to those described below.

As previously indicated, ISS telemetry bandwidth limitations do not favor the recording and post-analysis approach utilized by the STDCE. Crew time and experiment-specific expertise remain as scarce resources, creating the desire for rapid data analysis to assess possible changes in experimental parameters and/or configuration. With these issues in mind, current efforts emphasize direct digital transfer, increased analysis throughput, and continued reductions in spurious error rates. A hybrid processing architecture has been developed that combines the methods of cross-correlation and particle tracking.[14] This two-stage approach offers advantages of both methods. Principally, cross-correlation subregion analysis provides a five to ten-fold improvement in measurement accuracy, while the presence of displacement accuracy retains superior spatial resolution. More importantly, the resulting velocimetric technique is capable of addressing a broad range of seeding densities. This feature is extremely valuable for retrieving useful information from image fields or portions of image fields that would otherwise be unusable. Incorporated into the analysis are fuzzy logic algorithms which maximize the information recovery from the correlation operation, while reducing the occurrence of spurious vectors. Using these developments, analyses resulting in the correct identification of several thousand vectors have been implemented on conventional PC platforms with run times of the order of a minute. The data is acquired through a user friendly graphical interface and processed on-screen. This near real-time capability enables the operator to ensure that the experiment parameters (e.g. light sheet intensity, inter-exposure time, seeding density) are optimally set. The combined approach provides more than a threefold increase in spatial resolution of that obtained by cross-correlation alone. In related work, this method has been extended to obtain three component velocity information from stereoscopic data.[15]

4. Summary

The development of the International Space Station laboratory has spawned the need for measurement systems to support planned scientific investigations. Two categories of experimental studies baselined for initial deployment on the ISS concern the areas of combustion science and fluid physics. A primary attribute of these phenomena is the significantly diminished role of buoyancy-induced convective motions, the reduction of which is noticeably observed by differences in the resulting flow fields. These differences promote the requirement for suitable velocity field diagnostics.

The nature of the ISS laboratory places unique constraints not only on specific hardware elements, but on the methods in which experiments are conducted, data is acquired and analyzed, and refinements in subsequent experiments are deliberated and initiated. In this regard, the development of diagnostic capabilities emphasizes rapid analysis, minimization of transmitted telemetry packets, and robust parameter display and control.

References:

1. C. K. Law and G. M. Faeth, *Progress in Energy and Combustion Science*, vol. 20, pps. 65-113, 1994.
2. S. Ostrach, *Annual Review of Fluid Mechanics*, vol. 14, pps. 313-345, 1982.
3. R. J. Adrian, in Fluid Mechanics and Measurements, R. J. Goldstein, ed., Hemisphere Publishing, Washington, D.C., pps. 155-244, 1983.
4. I. Grant, *Proc. Instn Mech Engrs*, vol. 211, part C, pp 55-76, 1997.
5. W. M. Farmer, *Applied Optics*, vol. 11, pp. 2603-2609, 1972.
6. C. I. Moir, P. S. Greenberg, and A. McGregor, *Proceedings of the Optical Society of America Topical Meeting on Photon Correlation and Scattering*, 1996.
7. S. Hanson, *Journal of Physics D: Applied Physics*, vol. 6, pps. 164-171, 1973.
8. J. Mork, B. Tromberg and J. Mark, *Journal of Quantum Electronics*, vol. 28, no. 1, pps. 93-107, 1992.
9. J. J. Schneider, *Miniature and Micro Optics and Micromechanics*, SPIE vol. 1992, pps. 235-246, 1993.
10. H. Tan and J. Loh, *Optics and Lasers in Engineering*, 17, pps. 229-240, 1992.
11. M. P. Wernet and A. D. Pline, NASA Technical Memorandum 104482, 1991.
12. H. D. Ross and F. J. Miller, *Proceedings of The Twenty-Sixth Symposium (International) on Combustion*, pps. 1327-1334, 1996.
13. J. H. Wernet and M. P. Wernet, *Proceedings of the ASME Symposium on Laser Anemometry: Advances and Applications*, 1994.
14. M. P. Wernet, *SPIE Conference on Optical Diagnostics in Fluid and Thermal Flow*, vol. 2546, 1995.
15. M. P. Wernet, AIAA-96-2268, 1996.

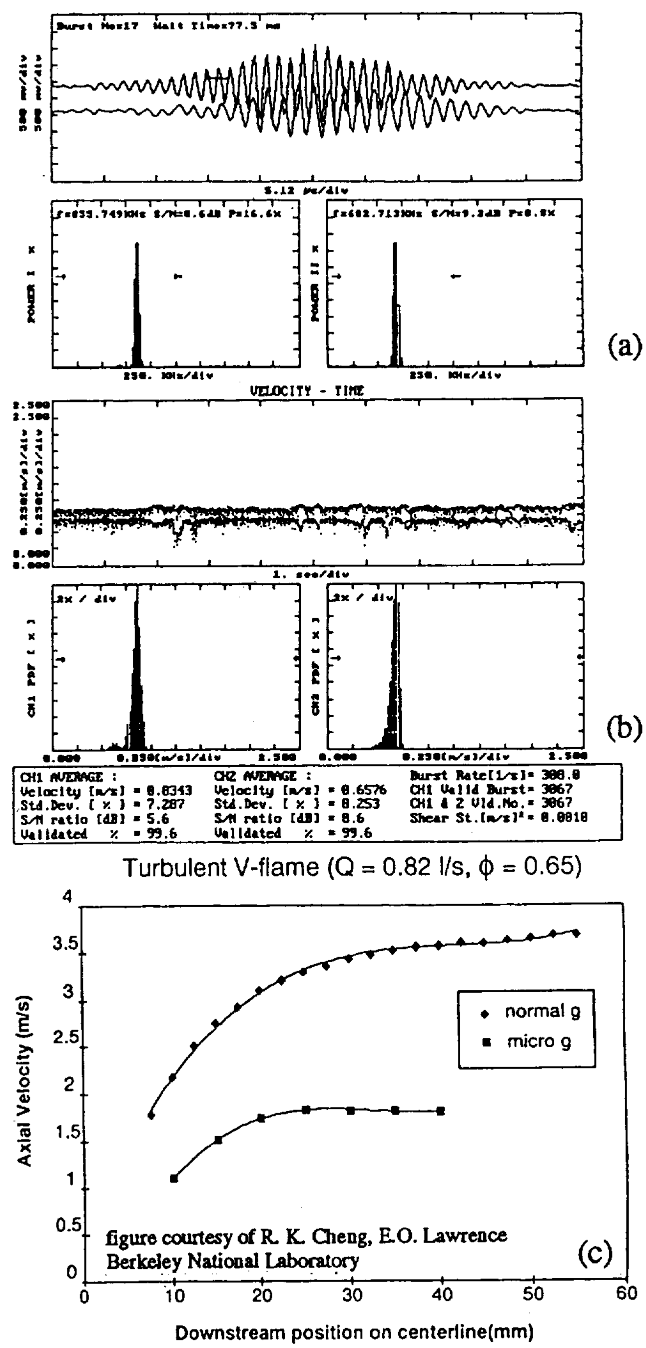

Figure 1

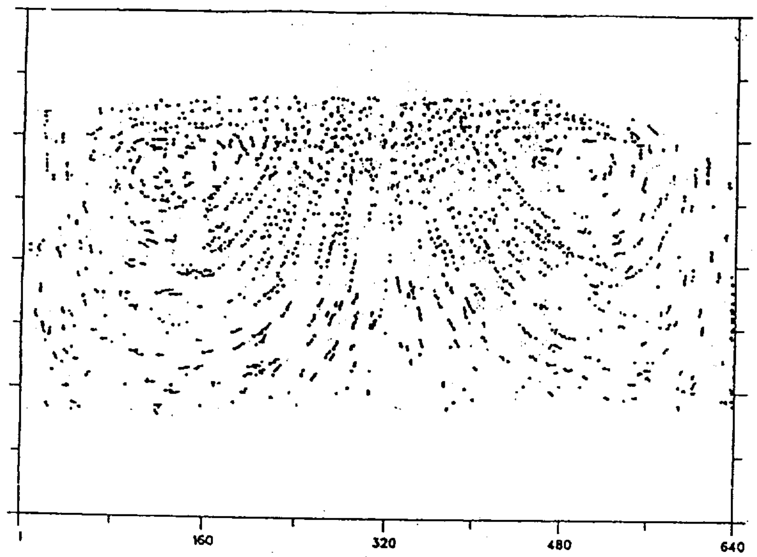

Time history coded particle image centroids plotted in pixel coordinates

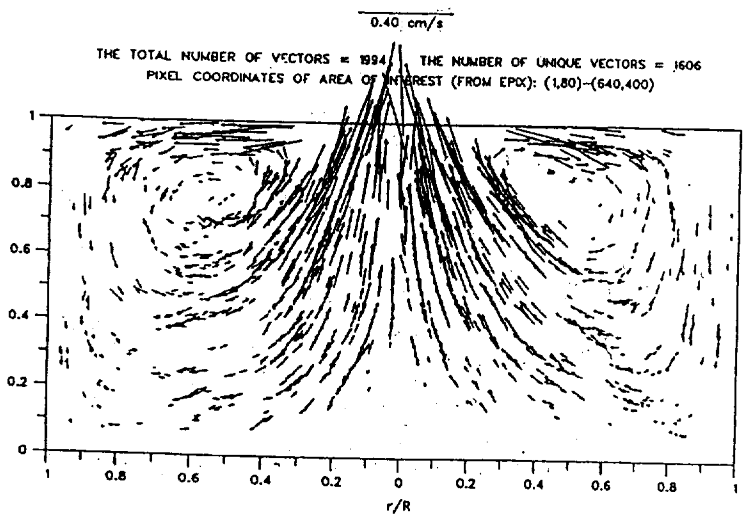

Velocity vector plot consisting of 6 combined data sets with false identifications removed

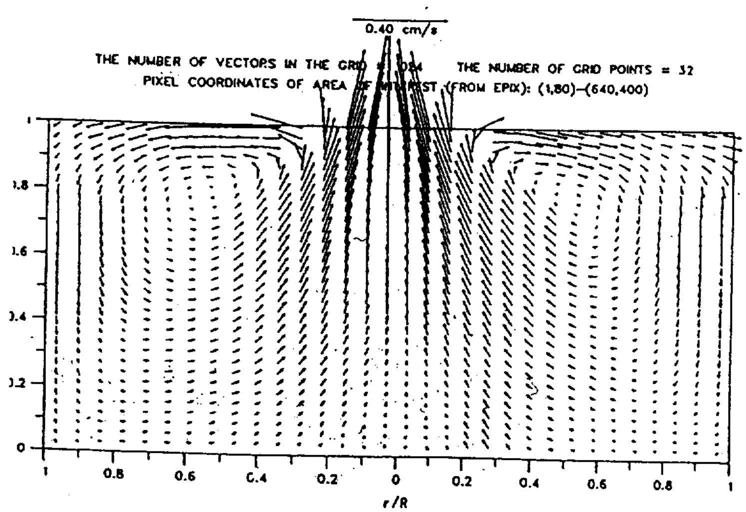

Interpolated 2-D velocity map in non-dimensional coordinates.

STDCE Particle Image Data

Figure 2